

Maximizing Multistage Turbine Efficiency by Optimizing Hub and Shroud Shapes and Inlet and Exit Conditions of Each Blade Row

Milan V. Petrovic¹, *Faculty of Mechanical Engineering, University of Belgrade, 27 Marta 80, 11000 Belgrade, Yugoslavia. Email: petr@afrodita.rcub.bg.ac.yu*

George S. Dulikravich² *, *Department of Mechanical and Aerospace Engineering, Box 19018, The University of Texas at Arlington, Arlington, TX 76019, U.S.A. Email: gsd@mae.uta.edu*

Thomas J. Martin³, *Department of Aerospace Engineering, 233 Hammond Building, Pennsylvania State University, University Park, PA 16802, U.S.A.*

Abstract

By matching a well established fast through-flow analysis code and an efficient optimization algorithm, a new design system has been developed which optimizes hub and shroud geometry and inlet and exit flow-field parameters for each blade row of a multistage axial flow turbine. The compressible steady state inviscid through-flow code with high fidelity loss and mixing models, based on stream function method and finite element solution procedure, is suitable for fast and accurate flow calculation and performance prediction of multistage axial flow turbines at design and significant off-design conditions. A general-purpose hybrid constrained optimization package has been developed that includes the following modules: genetic algorithm, simulated annealing, modified Nelder-Mead method, sequential quadratic programming, and Davidon-Fletcher-Powell gradient search algorithm. The optimizer performs automatic switching among the modules each time when the local minimum is detected thus offering a robust and versatile tool for constrained multidisciplinary optimization. An analysis of the loss correlations was made to find parameters that have influence on the turbine performance. By varying seventeen variables per each turbine stage it is possible to find an optimal radial distribution of flow parameters at the inlet and outlet of every blade row. Simultaneously, an optimized meridional flow path is found that is defined by the optimized shape of the hub and shroud. The design system has been demonstrated using an example of a single stage transonic axial gas turbine, although the method is directly applicable to multistage turbine optimization. The comparison of computed performance of initial and optimized design shows significant improvement in the multistage efficiency at design and off-design conditions. The entire design optimization process is feasible on a typical single-processor workstation.

Nomenclature

c	absolute velocity	Ma	Mach number
h	static enthalpy	\dot{m}	mass flow rate
h^0	total enthalpy	n	rotational speed (rpm)
\bar{h}	relative blade height, fraction of span	p	pressure
		R	Reynolds number
		s	entropy

¹ Associate Professor

² Professor, Author for correspondence.

³ Graduate Research Assistant.

T	temperature
t	blade pitch
u	tangential velocity
w	relative velocity
α	absolute flow angle (from tangential direction)
β	relative flow angle (from tangential direction)
δ	thickness, clearance height
ζ	loss coefficient
η	efficiency
Π	pressure ratio
ω	angular velocity (s^{-1})
ψ	stream function
θ	deflection angle

Subscripts

Cl	clearance
in	inlet
m	mean radius
out	outlet
r	radial component, reduced value
s	isentropic
tt	total to total
TE	Trailing edge
u	tangential component
z	axial component
1	stator outlet
2	rotor outlet

1. Introduction

Numerical optimization techniques may be successfully applied to different design problems. Especially, if the design target is a function of a large number of parameters, the optimization methods are highly recommended to use in order to find a combination of parameters giving the best solution. In the field of turbomachinery, efforts have been made to improve the aerodynamic performance, reduce the weight, and minimize production costs. The turbomachines should be designed for; the maximum possible mass flow rate per unit frontal area, the highest possible enthalpy change per rotor-stator stage, the minimum axial length, and the minimal number of blades per each

row. At the same time, the high aerodynamic efficiency at design conditions, acceptable performance at reasonable partial loads, and reliable operation for all expected conditions are required. Design methods, such as aerodynamic, thermal, and structural calculation procedures are applied by designers to determine suitable flow path geometry. All these methods may be coupled with procedures of numerical optimization to enable the variation of a large number of design parameters and an automatic determination of their best combination.

In recent years, a number of papers have been published on the application of optimization techniques in the design of turbomachines. Most of the early work has been done on optimization of 1-D pitchline design (for example, Balje and Binsley, 1968). This technique gives the optimum geometry of the row at mean diameter and is widely used for turbomachinery preliminary design. One-dimensional optimization does not provide any information concerning the three-dimensional shape of blade rows. Therefore, the introduction of 2-D and 3-D flow-field calculation methods providing more detailed information is necessary. To become suitable for applications in design optimization of multistage turbomachinery, the computational fluid dynamics (CFD) calculation codes should be sufficiently accurate and very fast. At the same time, optimization algorithms must be highly effective and reliable in order to keep the overall calculation time acceptable. Massardo *et al.* (1990) have presented a method for the design optimization of an axial flow compressor stage. Their procedure allows for optimization of a complete spanwise distribution of the blade geometry. Evaluation of the objective function (stage efficiency) was obtained with a through-flow code. The example given in their publication suggests that their approach may be used for design and redesign of axial compressor stages. Recently, Cravero and Dawes (1997) presented a concept for optimizing the design conditions of an axial turbine stage. The objective was to find such radial distribution of absolute swirl velocity at the inlet and exit of stator blade row and rotor blade row that will minimize the overall single stage losses.

They used a standard streamline curvature through-flow analysis code having standard loss correlations. A simple polynomial parameterization of the radial variation of swirl velocity and the stator and rotor lean angles was used. For optimization, they used a rudimentary gradient search constrained minimization routine.

In this paper, we will present our design approach that is capable of simultaneously optimizing the geometric and the flow-field parameters applicable to multistage axial flow turbomachines. The aerodynamic design optimization system is created by matching a well established and fast through-flow multistage analysis code and an efficient and robust hybrid constrained optimization algorithm. The method enables an automatic determination of the optimal radial distribution of flow angles at inlet and outlet of every blade row and an optimal shape variation of hub and shroud. The optimized solution provides for maximum multistage axial turbine efficiency. The design system will be demonstrated on an example of a single stage helicopter gas turbine. The comparison of computed performance of initial and optimized design shows significant improvement in the turbine efficiency.

The proposed design procedure, based on 2-D through-flow analysis code, has been envisioned as the second step in a turbine global design optimization process.

Using 1-D flow-field analysis in the first step, an experienced designer can obtain an initial meanline design.

In the second step, the proposed procedure delivers optimized meridional flow path and spanwise distribution of blades' inlet and outlet angles, pressures, and temperatures. This technique can utilize either an Euler or a Navier-Stokes based through-flow analysis code.

The third step would be a detailed 3-D inverse shape design or shape optimization of isolated stator and rotor blades' geometry subject to these optimized boundary conditions. Based on these new detailed blade shapes, it would be possible to repeat the second step and change the shape of the loss

coefficient radial profile thus further improving the turbine efficiency. It should be pointed out that the optimized radial distribution of the circumferential mean flow angles might not be realizable. In this case, the second design step could be repeated with modified constraints or the optimized radial distribution of flow parameters could be simplified in an *a posteriori* manner.

Simultaneous detailed fully 3-D aerodynamic shape optimization of all blade rows in a complete multistage turbine by applying a fully 3-D multistage turbulent compressible flow-field analysis code would be excessively time consuming even on an advanced multiprocessor computer. Consequently, our design optimization approach is suggested as an attractive cost-effective quasi 3-D alternative.

2. Through-Flow Code

The flow-field and performance of the axial turbine were calculated using a through-flow method developed by Petrovic (1995). This method is based on a classical through-flow theory (Hirsch and Deconinck, 1985), but includes some improvements and extensions. A finite element procedure with eight-node isoparametric quadrilateral elements and biquadratic interpolation functions was applied to solve the distribution of a stream function in a turbine meridional surface. It is basically an inviscid code with high fidelity distributed losses. The loss model developed by Traupel (1988) was adapted to 2-D calculations and applied in order to compute the loss coefficient and the entropy increase. This augmented through-flow method contains a model for realistic radial distribution of losses. An effective spanwise mixing model developed by Petrovic (1995) was introduced to avoid unrealistic entropy increase in the endwall zone of the blade row and to take into account radial energy transport due to secondary flow and turbulent mixing. All applied models (loss, deviation, radial loss distribution, and spanwise mixing) are based on a large amount of experimental data. These models account for all

major factors influencing the losses; consequently, they can predict main flow losses very well. More details about the analytical background of the method and applied loss and mixing model are given in a paper by Petrovic and Riess (1997b).

The through-flow code is able to calculate axisymmetric flow-fields in axial multistage gas turbines and steam turbines at subsonic and transonic conditions. It can accurately and very quickly predict the flow-field and the turbine performance at the design load as well as for a wide range of partial loads. Low load operation with flow reversal in the hub region behind the last rotor blade row and loads at which part of blading operates with power consumption may be also analyzed. The reliability of the method was verified by comparing the calculations with the experimental results for several gas and steam turbines (Petrovic and Riess, 1997a; 1997b). The comparisons of numerical results with results of extensive experimental investigation show very close agreement. The program can run on a typical PC or a workstation.

The through-flow code can be used in two modes: analysis and design mode. In the analysis mode, the flow-field (distribution of p , T , h , s and velocity vector components) on a meridional surface and turbine overall performance are calculated for the specified turbine geometry and fixed values of blade row inlet and outlet angles. For optimization purposes, the through-flow code has been rewritten in a design mode, in which the radial distribution of the tangential velocity component is fixed. The flow angle and turbine efficiency can then be calculated.

3. Optimization

The goal of the presented optimization is to find optimal turbine geometry (shape of hub and shroud and radial distribution of inlet and outlet angles of every blade row) giving the maximum

turbine efficiency η_u ($\eta_u = (\Delta h + c_{in}^2/2 - c_{out}^2/2) / (\Delta h_s + c_{in}^2/2 - c_{out}^2/2)$). Since optimization algorithm is defined to minimize a function, the objective function in our case is: $f_{obj} = -\eta_u$. During the geometry optimization process, turbine mass flow rate \dot{m} , total enthalpy drop Δh^0 , and rotational speed n will be kept constant.

3.1. Design Variables

We have applied an updated version of Traupel's loss model that was adapted for 2-D flow calculation. In this model, the correlations for profile, secondary, and clearance losses are functions of geometrical and flow parameters.

The analysis of loss correlations shows that turbine stage efficiency is a function of geometric parameters (mean radius R_m , blade height h , pitch t , clearance radius R_{Cl} and height δ_{Cl} , trailing edge thickness δ_{TE} , chord length) and flow parameters (inlet and outlet flow angles: β_1 , β_2 , deflection θ , Mach and Reynolds numbers Ma , Re , incidence angle, and velocity vectors). Some of these parameters (δ_{Cl} , δ_{TE}) have to be fixed. The others are not independent: velocities, Ma , and Re are functions of flow angles. Also, inlet angle is a function of the outlet angle of the previous row and of the incidence angle.

Consequently, the radial distribution of four parameters needs to be optimized for each stage of the multistage turbine:

- $\alpha_1(R)$ – stator outlet angle,
- $\beta_2(R)$ – rotor outlet angle,
- $h(z)$ – blade height,
- $R_m(z)$ – blade mean radius.

However, it is easier to optimize the radial variation of the following four parameters per each stage of the multistage machine:

- $c_{u1}(R)$ – tangential component of velocity at stator outlet,

- $c_{u2}(R)$ - tangential component of velocity at rotor outlet,
- $R_{Hub}(z)$ - hub radius,
- $R_{Shroud}(z)$ - shroud radius.

Once the optimized values of $c_{u1}(R)$ and $c_{u2}(R)$ are known, the corresponding optimized spanwise distribution of angles is easy to calculate.

The axial distribution of hub and shroud radii can be successfully described by two spline functions, $R_{Hub}(z)$ and $R_{Shroud}(z)$. The radial coordinates of points at inlet and outlet of stator and rotor on hub and shroud surfaces are introduced as spline function parameters. For simplicity, we decided to use only four geometrical parameters per every stage for hub and four geometrical parameters per every stage for shroud (Fig. 1). If desired, this can be easily changed to an arbitrarily complex spline representation of the hub and shroud.

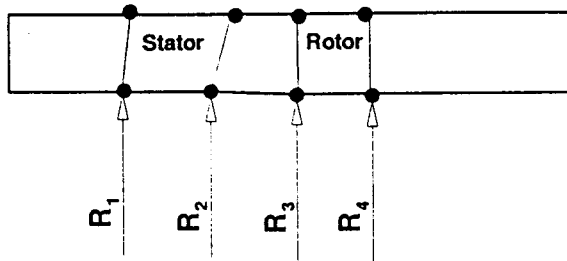


Fig. 1: Geometric design variables for the hub.

Tangential components of velocities at stator and rotor outlet were described by polynomials of the fourth degree as a function of relative blade height ($0.0 < \bar{h} < 1.0$). This representation needs the following 10 parameters:

$$c_{u1} = A_1 + B_1\bar{h} + C_1\bar{h}^2 + D_1\bar{h}^3 + E_1\bar{h}^4 \quad (1)$$

$$c_{u2} = A_2 + B_2\bar{h} + C_2\bar{h}^2 + D_2\bar{h}^3 + E_2\bar{h}^4 \quad (2)$$

One of these 10 parameters can be obtained using condition $\Delta h^0 = const.$ This means that the integral of Euler equation over mass flow rate has to be constant for every combination of flow and geometric parameters.

$$\Delta h^0 = \int_0^1 (u_1 c_{u1} - u_2 c_{u2}) d\psi = const. \quad (3)$$

Replacing c_{u1} and c_{u2} by functions (1) and (2), we obtain

$$\Delta h^0 = A_1 \omega [I_1 - I_2] \quad (4)$$

$$I_1 = \int_0^1 R \left(1 + \frac{B_1}{A_1} \bar{h} + \frac{C_1}{A_1} \bar{h}^2 + \frac{D_1}{A_1} \bar{h}^3 + \frac{E_1}{A_1} \bar{h}^4 \right) d\psi \quad (5)$$

$$I_2 = \int_0^1 R \left(\frac{A_2}{A_1} + \frac{B_2}{A_1} \bar{h} + \frac{C_2}{A_1} \bar{h}^2 + \frac{D_2}{A_1} \bar{h}^3 + \frac{E_2}{A_1} \bar{h}^4 \right) d\psi \quad (6)$$

$$A_1 = \frac{\Delta h^0}{\omega (I_1 - I_2)} \quad (7)$$

where I_1 and I_2 are the values of the integrals in eqns. (5)-(6). Stream function ψ and radius R are functions of relative blade height \bar{h} .

Hence, there are 9 flow parameters to optimize the tangential components of velocities at stator and rotor outlets:

$$\frac{B_1}{A_1}, \frac{C_1}{A_1}, \frac{D_1}{A_1}, \frac{E_1}{A_1}, \frac{B_2}{A_1}, \frac{C_2}{A_1}, \frac{D_2}{A_1}, \frac{E_2}{A_1} \quad (8)$$

In summary, the total number of parameters to optimize for every turbine stage is 17 (8 geometrical and 9 flow parameters).

3.2 Constrained Hybrid Optimization Algorithm

The design space for a typical optimization problem of this type has a number of local minimas (Foster and Dulikravich, 1997). A typical gradient based optimization algorithm would quickly terminate in the nearest available local minimum which might not even satisfy all of the specified

constraints (Foster and Dulikravich, 1997). In order to avoid the local minimums, it is advantageous to use a constrained evolutionary hybrid optimization approach (Foster and Dulikravich, 1997; Martin and Dulikravich, 1997; Dulikravich *et al.* 1998; Dulikravich *et al.* 1999). The hybrid constrained algorithm used in this work incorporated four of the most popular optimization approaches: a genetic algorithm (GA), the Nelder-Mead (NM) simplex method, simulated annealing (SA), and Davidon-Fletcher-Powell (DFP) gradient search method (Haftka and Gurdal, 1992). Each technique separately provided a unique approach to optimization with varying degrees of convergence, reliability, and robustness at different stages during the iterative optimization procedure. Each time when a local minimum was detected, an automatic switching logic was used to change to another optimization algorithm. The optimization problem was completed when every optimizer failed to arrive at a better design simultaneously. This usually indicated that a global minimum had been found (Martin and Dulikravich, 1997).

Unfortunately, in this hybrid optimization approach which only occasionally uses gradients of the objective function, it is practically impossible to determine the sensitivity of turbine efficiency with respect to each of the design parameters. The hybrid optimizer treated the existence of constraints in three ways: Rosen's projection method, a feasible search, and random design generation. Rosen's projection method (Haftka and Gurdal, 1992) provided search directions which guided the descent direction tangent towards active constraint boundaries. In the feasible search, designs that violated constraints were automatically restored to feasibility via the minimization of the active global constraint functions. If at any time this constraint minimization failed, a number of random designs were generated using a Gaussian-shaped probability density cloud about a desirable and feasible design until a new design was reached. This hybrid constrained optimizer accepts an arbitrary number of equality and inequality constraints. In its present version, it cannot perform multipoint (multiobjective) constrained optimization.

3.3 Optimization Strategy

The general optimization algorithm is presented in Fig. 2. The first optimization cycle (iteration) starts from initial turbine geometry and input flow data: \dot{m} , T_{in} , p_{in} . Through-flow code in analysis mode provides evaluation of overall performance of the initial configuration and initiates the distribution of c_{u1} and c_{u2} . The optimizer then delivers an improved set of geometrical (shapes of hub and shroud) and flow (distribution of c_{u1} and c_{u2} parameters. A new finite element grid is then automatically generated for the meridional flow-field surface. The through-flow code in its design mode then runs with the new distributions of c_{u1} and c_{u2} thus creating a new set of flow parameters. The result is the spanwise distribution of flow angles at inlet and outlet of every blade row, and the overall turbine efficiency. Depending on the achieved η , the optimizer enters the next iterative cycle by generating a new set of parameters and the iterative optimization process is repeated until the maximum

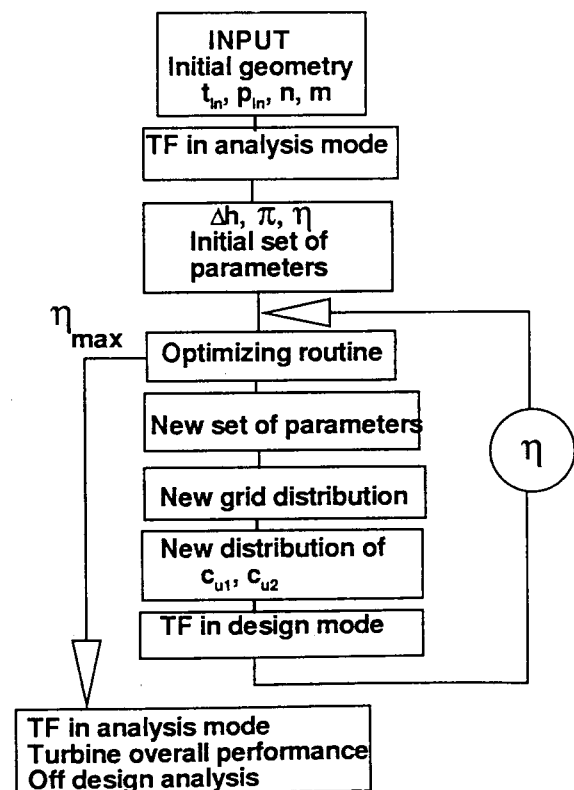


Fig. 2: Optimization algorithm scheme.

of efficiency is achieved.

By running the through-flow code in its analysis mode, the overall efficiency of the optimal configuration over a wide range of part loads is then calculated in order to check the optimized turbine off-design performance. If the overall efficiency of the optimal configuration at all expected operating conditions is acceptable, the optimization process is finished.

The iterative design process runs fully automatically. The designer's task is to prepare the input data and to set constraints for design variables. The flow variables are usually allowed to vary without any limits. The variation of the rotor blade tip radius is often limited by the maximum stress at the rotor root, that is, by the maximum allowed tangential velocity if the rotating speed is fixed.

4. Example of an Application

Due to the lack of availability of detailed experimental data for a truly multistage axial gas turbine, the single stage uncooled turbine described by Foerster and Kruse (1990) was selected for verification of the presented optimization process. The turbine represents a test version of the first stage of a helicopter engine turbine. This well-documented set of experimental data (Foerster and Kruse, 1990), has been used to check the numerical results. The nominal rotational speed for this gas turbine is $n = 7800.0 \text{ rpm}$ ($n_r = 0.99679 \text{ s}^{-1} \text{ K}^{-0.5}$). The reduced mass flow rate is $\dot{m} \sqrt{T} / p = 97.0 \text{ kg K}^{0.5} \text{ s}^{-1} \text{ bar}^{-1}$, and reduced total enthalpy drop is $\Delta h^0 / T = 135.0 \text{ J kg}^{-1} \text{ K}^{-1}$. The tip radius is 0.225 m and hub-to-tip radius ratio is 0.756. Static tip clearance of the rotor is 0.25 mm. The stator does not have any tip clearance.

To check the through-flow code in analysis mode, the calculation of the turbine overall performance (reduced mass flow rate, $\dot{m} \sqrt{T} / p$, and turbine efficiency, η_u , as functions of reduced total enthalpy drop, $\Delta h^0 / T$), has been performed and compared with available experimental data (Foerster and Kruse, 1990) at the reduced rotating speed $n_r =$

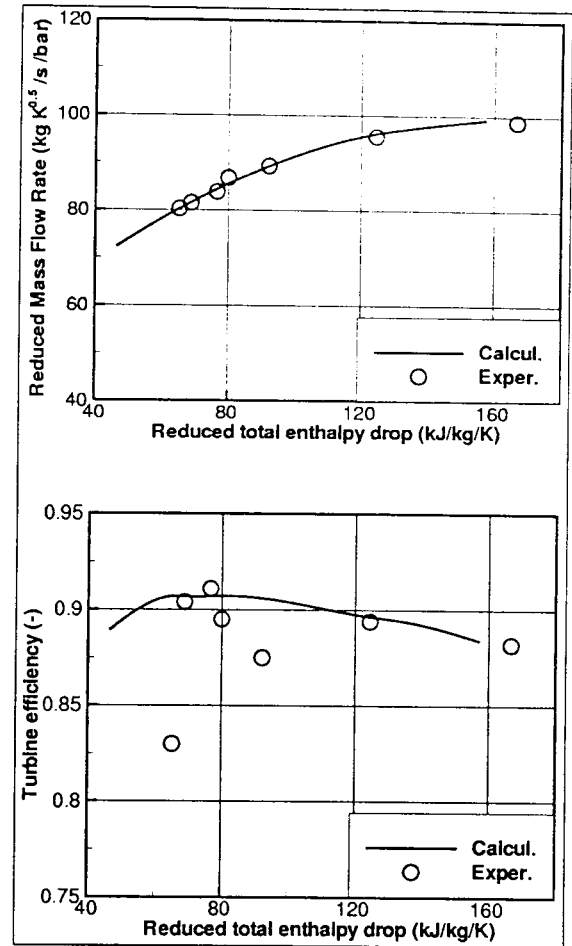


Fig. 3: Overall performance of the single stage.

$6.833 \text{ s}^{-1} \text{ K}^{-0.5}$ (Fig. 3). The design value was something higher ($n_r = 6.9679 \text{ s}^{-1} \text{ K}^{-0.5}$). The comparison of calculations with experiments shows good agreement. The computed and measured radial distributions of total temperature and total pressure at stator (SE) and rotor (RE) exit at design point are shown in Fig. 4. At the design conditions the calculated value of turbine efficiency was $\eta_u = 0.8952$, while the measured $\eta_u = 0.8940$.

The optimization was performed while keeping constant rotational speed, mass flow rate, total enthalpy drop, number of blades, rotor tip clearance, blade chord lengths, and blade trailing edge thicknesses. There was only one geometric constraint in this test case: blade tip radius was allowed to change its value up to 0.2275 m (initial value was 0.225 m). It was assumed that both blade

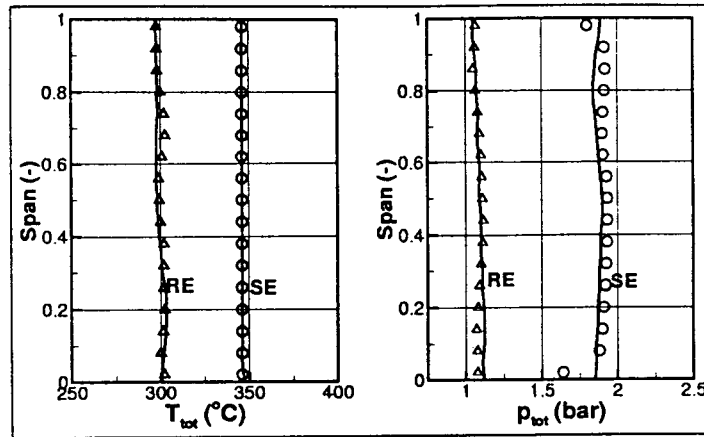


Fig. 4: Radial variation of total temperature and total pressure at stator exit (SE) and rotor exit (RE) of the single-stage turbine at design condition: numerical results (lines); experimental data (symbols).

count and chord lengths have been already determined by some preliminary design procedure (for example, meanline optimization as the first design step). In principle, it is possible to include both of these parameters (and other parameters deemed to be influential) in this optimization method. Obviously, this would result in more than 17 design parameters per stage to be optimized.

The through-flow code in its design mode needed approximately 18 seconds to find each flow-field solution. To find the turbine stage configuration that gives the maximum total-to-total efficiency, three optimization cycles (each requiring 17 through-flow runs in the design mode) were necessary in this test case when using DFP optimizer. The entire design optimization process took 15 minutes on an SGI R10000 workstation. The small number of optimization cycles used in this example indicates that a local minimum rather than the global minimum was reached. This suggests that even better result could have been achieved if other optimization algorithms (especially those that are not based on gradient search) have been utilized. Nevertheless, use of the semi-stochastic optimizers (GA, NM, SA) would require significantly more calls to the through-flow analysis module thus consuming potentially significantly more computer time (Foster and Dulikravich, 1997).

The maximum achieved value for the turbine

efficiency is: $\eta_{tt} = 0.9154$. Comparing to the efficiency of the initial configuration ($\eta_{tt,init} = 0.8952$), the absolute improvement is approximately $\Delta\eta_{tt} = 2.0\%$. Figure 5 shows the overall performance of the optimized configuration (OC) and a comparison with the performance of the initial configuration (IC). The efficiency of the OC is better over the wide range of loads ($50 < \Delta h^0 / T < 150$).

The drop of η_{tt} in OC case starts at some higher loads. Depending on turbine application, this can be a disadvantage of this particular solution. In that case, some changes in constraints can be undertaken to insure better behavior at the part loads.

Figure 6 shows a comparison of meridional flow paths for OC and IC. The changes are relatively small. However, these changes of hub and shroud shapes together with the new distribution of angles at inlet and outlet of the stator and the rotor have as a result a significant decrease in the flow losses and the entropy generation. Comparisons of spanwise distributions of blade exit metal angles, flow losses, reaction, stage efficiency, and different flow-field parameters for the initial and the optimized configuration are presented in Fig. 7 and Fig. 8. Figure 9 shows the computed flow-field entropy distribution in the initial and the optimized configuration. It can be seen that it was not possible to reduce the flow loss coefficient in the stator (Fig.

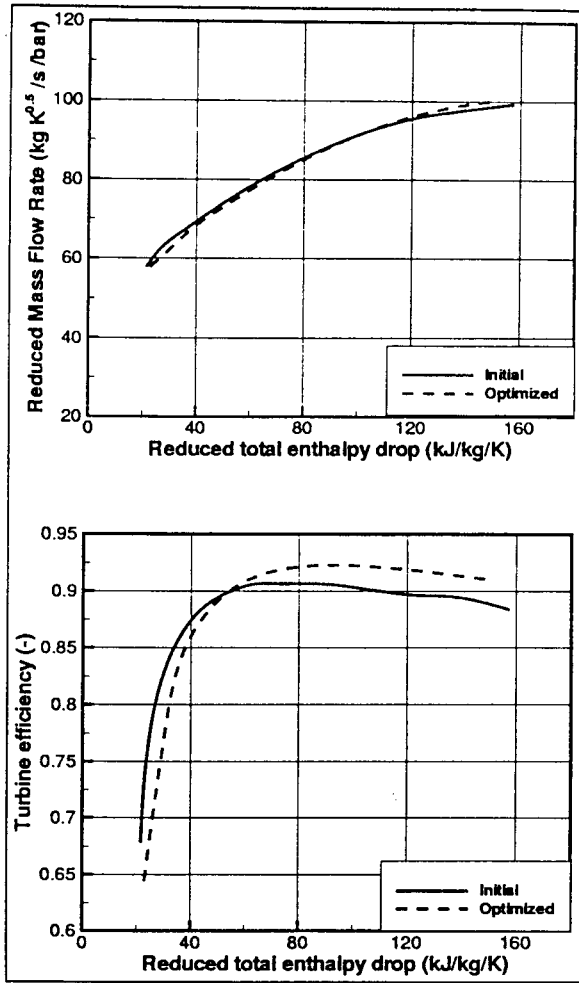


Fig. 5: Overall performance of initial and optimized configuration at design rotating speed. (Design reduced total enthalpy drop $\Delta h^0 / T = 132,000 \text{ J kg}^{-1} \text{ K}^{-1}$)

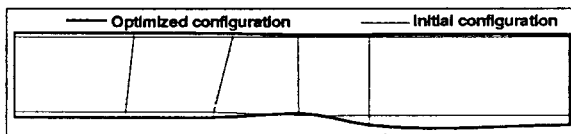


Fig. 6: Comparison of initial and optimized meridional flow paths.

7) since the flow at its inlet was specified and only small changes in the stator outlet flow angles were made. But, the flow losses and the entropy increase have been reduced (Fig. 9) by decreasing the

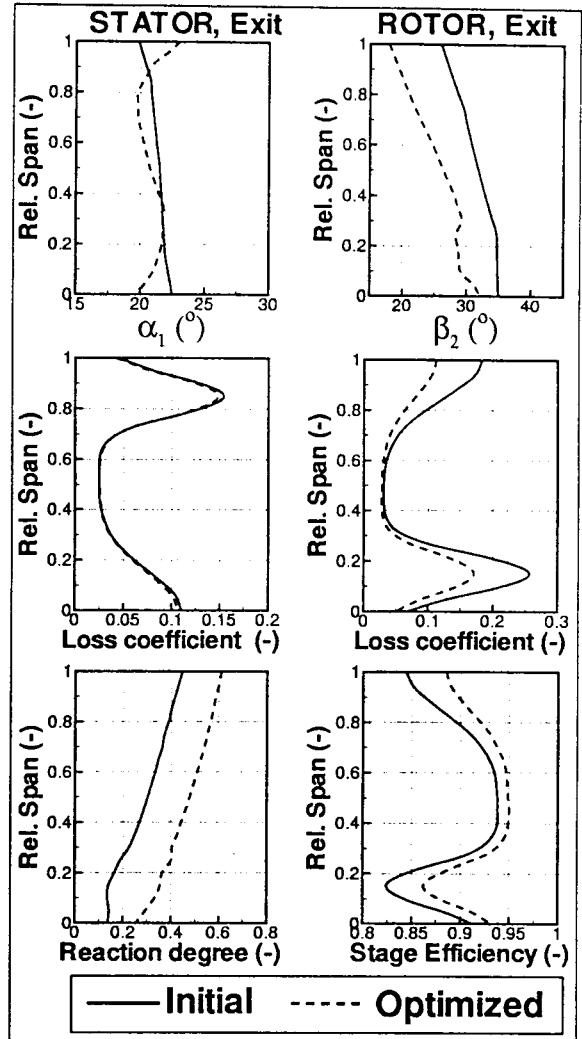


Fig. 7: Spanwise distribution of blade exit metal angles, flow losses, reaction, and stage efficiency in the initial and the optimized configuration.

velocity at the stator exit (Fig. 8). The degree of reaction has been increased so that the optimized configuration has the degree of reaction of approximately 0.5 at the blade mean radius. Also, axial velocities (Fig. 8) in the endwall zones that have strong secondary flows and clearance losses were additionally reduced in order to minimize the mass flow through this part of the flow path.

The reduction of loss coefficient in the rotating blade row, especially in the endwall zones was significant (Fig. 7). This was possible since inlet and

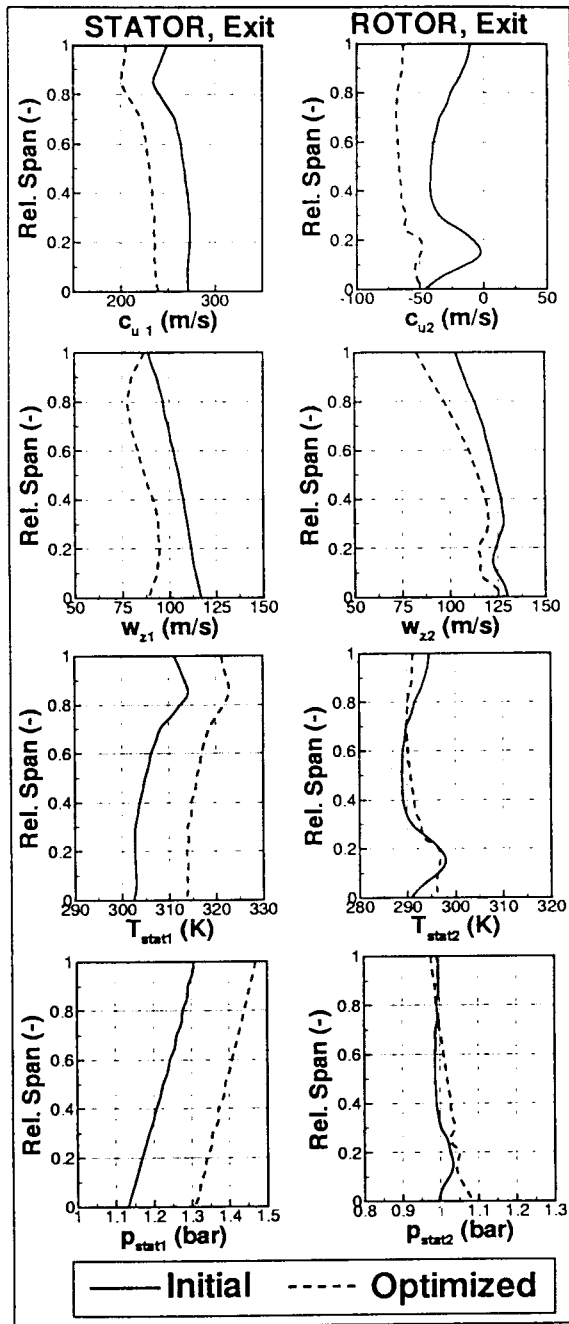


Fig. 8: Comparison of flow parameters over the blade span in the initial and the optimized stage configuration.

outlet flow was allowed to vary. All these changes of geometry and flow parameters at inlet and outlet of the blade rows result in increase of stage efficiency (Fig. 7). The largest improvement was

achieved in the endwall zones. The improvement of stage efficiency in the mean part of the turbine was realized by a more suitable distribution of enthalpy drop between stator and rotor thus creating a higher degree of reaction.

Conclusions

The design system for multistage axial turbine geometry optimization has been developed. The system matches a fast and accurate through-flow aerodynamics code and an effective constrained optimization package. The analysis of loss models has indicated that there are 17 parameters per every turbine stage that could be optimized. Eight geometrical parameters were used to describe, by means of a spline function, the shape of hub and shroud. Nine flow-field parameters were used to describe, using 4th degree polynomials, the tangential component of velocity at stator and rotor exits. By varying these 17 parameters per turbine stage, the optimizer searches the flow-field and the turbine hub and shroud geometry that gives the maximum efficiency.

The design system has been successfully applied to optimization of the meridional flow path and radial distribution of circumferential mean flow angles in a single stage turbine assuming very high fidelity loss and mixing models. The achieved efficiency of the optimized configuration was 2% better than the efficiency of the initial configuration at the design load. Possibly an even better result could have been obtained if we had to optimize a stage with stator clearance and were allowed to change stator inlet angles. Through-flow code in an analysis mode was applied to analyze off-design behavior of the optimized configuration which was found to perform better over a wide range of loads compared to the initial configuration. The optimization process runs fully automatically and it takes less than 15 minutes on a standard workstation to find an optimized solution in the considered example. The same procedure is applicable for multistage gas and steam turbines. Further improvement of turbine efficiency is possible by 3-D

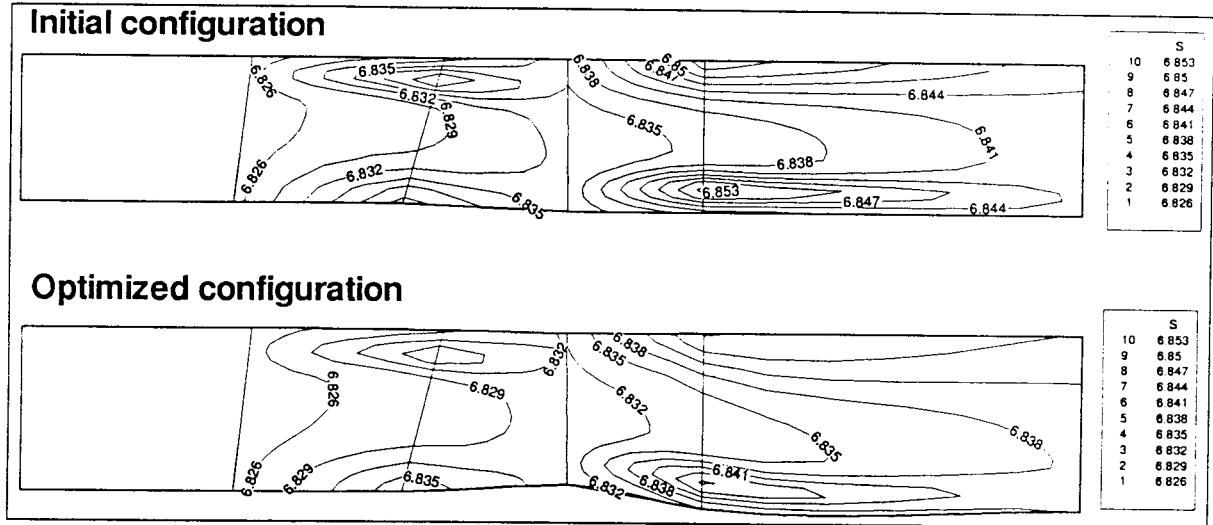


Fig. 9: Calculated entropy distribution in initial and optimized single stage axial gas turbine configuration.

inverse shape design of isolated stator and rotor blades geometry subject to the optimized inlet and exit boundary conditions of each blade row.

Acknowledgements

The authors are grateful for National Science Foundation Grant, DMI-9522854 and DMI-9700040 monitored by Dr. George Hazelrigg and for NASA Lewis Research Center Grant NAG3-1995 facilitated by Dr. John Lytle and supervised by Dr. Kestutis Civinskas.

References

- Balje, O. and Binsley, H., 1968: "Axial Turbine Performance Evaluation", *ASME Journal of Engineering for Power*, Vol. 90, pp. 341-360.
- Cravero, C. and Dawes, W. N., 1997: "Throughflow Design Using An Automatic Optimisation Strategy", *42nd International Gas Turbines and Aeroengines Congress*, Orlando, Florida, U.S.A., June 2-5, 1997, ASME Paper No. 97-GT-294.
- Dulikravich, G. S., Martin, T. J., Dennis, B. H., Lee, E.-S. and Han, Z.-X., 1998: "Aero-Thermo-Structural Design Optimization of Cooled Turbine Blades," AGARD - AVT Propulsion and Power Systems Symposium on Design Principles and Methods for Aircraft Gas Turbine Engines, NATO-RTO-MP-8 AC/323 (AVT)TP/9, Ch. 35, Toulouse, France, May 11-15, 1998.
- Dulikravich, G. S., Martin, T. J., Dennis, B. H. and Foster, N. F., 1999: "Multidisciplinary Hybrid Constrained GA Optimization", Invited lecture, Chapter 12 in *EUROGEN'99 - Evolutionary Algorithms in Engineering and Computer Science: Recent Advances and Industrial Applications*, (editors: K. Miettinen, M. M. Makela, P. Neittaanmaki and J. Periaux), John Wiley & Sons, Ltd., Jyvaskyla, Finland, May 30 - June 3, 1999, pp. 231-260.
- Foerster, W. and Kruse, H., 1990: "Test Case E/TU-3, Single Stage Subsonic Turbine", in *AGARD AR 275: Test Cases for Computation of Internal Flows in Aero Engine Components*, (editor: Fottner, L.)
- Foster, N. F. and Dulikravich, G. S., 1997: "Three-Dimensional Aerodynamic Shape Optimization Using Genetic and Gradient Search Algorithms", *AIAA Journal of Spacecraft and Rockets*, Vol. 34, No. 1, pp. 36-42.

- Haftka, R. T. and Gurdal, Z., 1992: *Elements of Structural Optimization*, 3rd edition, Kluwer Academic Publishers, Boston, MA.
- Hirsch, C. and Deconinck, H., 1985: "Through Flow Models for Turbomachines: Stream Surface and Passage Averaged Representations" in: *Thermodynamics and Fluid Mechanics of Turbomachinery*, Vol. I, (editors: Ucer, A. S., Stow, P., and Hirsch, C.), Martin Nijhoff Publishers, Dordrecht, The Netherlands.
- Martin, T. J. and Dulikravich, G. S., September 1997: "Aero-Thermal Analysis and Optimization of Internally Cooled Turbine Blades", *XIII International Symposium on Airbreathing Engines (XIII ISABE)*, Chattanooga, Tennessee, U.S.A., ISABE 97-7165, Vol. 2, pp. 1232-1250.
- Massardo, A., Satta, A. and Marini, M., 1990: "Axial Flow Compressor Design Optimisation: Part II -- Throughflow Analysis", *ASME Journal of Turbomachinery*, Vol. 112, July 1990, pp. 406-410.
- Petrovic, M. V. and Riess, W., 1995: "Through-Flow Calculation in Axial Flow Turbines at Part Load and Low Load", *1st European Conference 'Turbomachinery - Fluid Dynamic and Thermodynamic Aspects*, Erlangen, Germany.
- Petrovic, M. V., 1995: "Berechnung der Meridianstroemung in mehrstufigen Axialturbinen bei Nenn- und Teillastbetrieb", *Fortschritt-Berichte VDI, Reihe 7: Stroemungstechnik*, No. 280, VDI-Verlag, Dusseldorf, Germany.
- Petrovic, M. V. and Riess, W., 1997a: "Off-Design Flow Analysis of LP Steam Turbines", *2nd European Conference on Turbomachinery - Fluid Dynamic and Thermodynamic Aspects*, Antwerpen, Belgium, March 5-7, 1997.
- Petrovic, M. and Riess, W., 1997b: "Off-Design Flow Analysis and Performance Prediction of Axial Turbines", *42nd International Gas Turbines and Aeroengines Congress*, Orlando, Florida, U.S.A., June 2-5, 1997, ASME Paper No. 97-GT-55.
- Traupel, W., 1988: *Thermische Turbomaschinen*, Vol. I, Springer-Verlag, Berlin.